Scheme to generate continuous-variable quadripartite entanglement by intracavity down-conversion cascaded with double sum-frequency generations

H. Y. Leng, J. F. Wang, Y. B. Yu, X. Q. Yu, P. Xu,* Z. D. Xie, J. S. Zhao, and S. N. Zhu†
Department of Physics, National Laboratory of Solid State Microstructures, Nanjing University, Nanjing 210093, People's Republic of China
(Received 20 November 2008; published 27 March 2009)

We theoretically show that continuous-variable genuine quadripartite entanglement can be generated by intracavity cascaded nonlinear optical interactions. The process consists of a parametric down-conversion, a sum-frequency generation of pump and signal and a sum-frequency generation of pump and idler. The characteristics of the quadripartite entanglement among the signal, the idler, and two sum-frequency modes are analyzed by applying a sufficient inseparability criterion for multipartite continuous-variable entanglement proposed by Van Loock and Furusawa. The threshold properties of the system are also discussed.

DOI: 10.1103/PhysRevA.79.032337 PACS number(s): 03.67.Bg, 42.65.Lm, 42.50.Dv, 03.67.Mn

I. INTRODUCTION

Quantum entanglement is one of the most mysterious quantum phenomena and has become an indispensable resource for quantum information today. In recent years much effort has been devoted into the study of continuous-variable (CV) quantum communication network [1–4], the base of which is multipartite entanglement. Up to now, multipartite CV entanglement usually has been obtained by two methods. One is to mix squeezed beams on unbalanced beam splitters [1,2,5,6], but this method can produce only entanglement of modes with the same frequency because the beam splitter transformation is linear. The other way is to employ nonlinear optical processes, by which entanglement of modes with different frequencies can be produced. It enables transmitting, storing, and processing quantum information via different frequency bands in the quantum communication network [7]. Over the past several years, generation of CV tripartite entanglement by cascaded or concurrent nonlinear optical processes has been investigated extensively [8–12]. In particular, an intracavity process combining a parametric down-conversion with a sum-frequency generation has attract much interest [8–11]. Actually the process can be experimentally realized with quite a high efficiency [13]. Based on this process, we propose a scheme to generate CV genuine quadripartite entanglement by intracavity down-conversion cascaded with double sum-frequency generations. Unlike the quadripartite entanglement states obtained using linear optics [14], quadripartite entanglement of modes with four different frequencies can be produced by this scheme. The scheme can be realized in a one-sided optical cavity, in which a triperiodic or quasiperiodic optical superlattice is used as the nonlinear medium. In our scheme, only one pump is needed. After the signal and the idler are generated by a parametric down-conversion in the superlattice, the third beam is generated by a sum-frequency generation of the pump and the signal, and the fourth beam by a sum-frequency generation of the pump and the idler. The phase mismatching in these nonlinear processes can be compensated by three independent reciprocals of the triperiodic or quasiperiodic superlattice in quasi-phase-matching (QPM) scheme. For example, we may design a scheme with a 980 nm pump down-converted to signal and idler at 1318 and 3822 nm, respectively. The wavelengths of the two sum-frequency beams are then centered at 562 and 780 nm, respectively. In this scheme, the signal at 1318 nm is suitable to be transmitted through optical fibers over long distances and 780 nm is one of the absorption lines of the rubidium atom considered useful for the storage and processing of quantum information. The phase mismatching in above three processes can be compensated at 180 °C in QPM scheme by reciprocals of a triperiodically poled lithium tantalate with three periodically poled structures set in tandem of period 26.9, 9.0, and 21.6 μm, respectively. Triperiodically poled lithium niobate or potassium titanium oxygenic phosphate (KTP) are also good candidates for the nonlinear medium in our QPM scheme. In this work, CV genuine quadripartite entanglement is theoretically demonstrated among the signal, the idler and two sum-frequency modes. Owing to the flexibility of QPM scheme, almost any desired wavelengths of the entangled four modes can be obtained by modifications of phase-matching conditions and the pump wavelength. The entanglement characteristics and threshold properties of the system are also analyzed.

The paper is arranged as follows. A physical system for CV quadripartite entanglement generation is discussed in Sec. II. The threshold properties of the system are discussed and the output fields are derived in Sec. III. The entanglement characteristics of the four nonpump modes are analyzed in Sec. IV. Finally, we shall give a brief conclusion.

II. CASCADED NONLINEAR INTERACTION

In this work, we consider a one-sided optical oscillator cavity which is driven by an external, stationary, and coherent pump field with frequency ω_0 [Fig. 1(a)]. The QPM schematic of three nonlinear processes realized in the optical superlattice is plotted in Fig. 1(b). In the first step, two beams of frequency ω_1 and ω_2 are generated by a parametric down-conversion (PDC). In the second step, a third beam of fre-

*pingxu520@gmail.com
†zhusn@nju.edu.cn

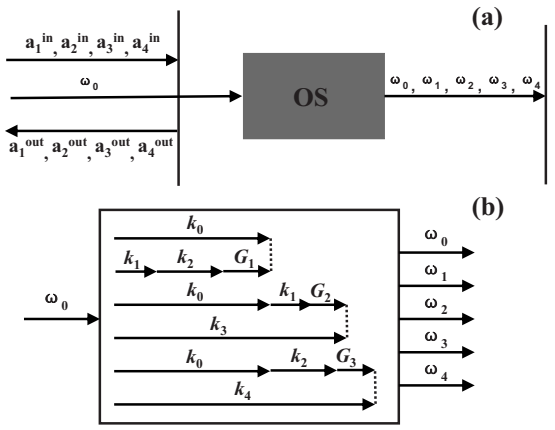

FIG. 1. (a) Sketch of the one-sided optical oscillator cavity driven by an external, stationary, and coherent pump field with frequency ω_0. An optical superlattice (OS) in the optical cavity is used to realize the cascaded nonlinear interactions. Four modes of light fields with frequency ω_1, ω_2, ω_3, and ω_4 are generated in the cavity. α_i^{in} $(i=1,2,3,4)$ and α_i^{out} $(i=1,2,3,4)$ are corresponding input and output fields of these four modes. (b) The QPM schematic for the cascaded nonlinear interactions. k_0, k_1, k_2, k_3, and k_4 are the corresponding wave vectors of pump ω_1, signal ω_1, idler ω_2, and two sum-frequency fields ω_3, ω_4. G_1, G_2, and G_3 are three independent reciprocals provided by the optical superlattice.

quency ω_3 is produced by a sum-frequency generation of the pump ω_0 and the beam ω_1 (SFG1), on the other hand, a fourth beam of frequency ω_4 is produced by a sum-frequency generation of the pump ω_0 and the beam ω_2 (SFG2). k_0, k_1, k_2, k_3, and k_4 are the corresponding wave vectors of pump, signal, idler, and two sum-frequency beams, respectively. In order to fulfill the above cascaded nonlinear processes in a single nonlinear medium, we can design a triperiodic or quasiperiodic optical superlattice. Such a superlattice is able to provide three independent reciprocals, G_1, G_2, and G_3, which can compensate the phase mismatching of PDC, SFG1, and SFG2 in QPM scheme. The reciprocal vector G_1 is used for PDC, G_2 for SFG1, and G_3 for SFG2, respectively. The energy conservation and phase-matching conditions are $\omega_0=\omega_1+\omega_2$, $\Delta k_{\mathrm{PDC}}=k_0-k_1-k_2-G_1=0$ for PDC, $\omega_0+\omega_1=\omega_3$, $\Delta k_{\mathrm{SFG1}}=k_3-k_0-k_1-G_2=0$ for SFG1, and $\omega_0+\omega_2=\omega_4$, $\Delta k_{\mathrm{SFG2}}=k_4-k_0-k_2-G_3=0$ for SFG2, respectively. In this work we assume that the pump, signal, idler, and two sum-frequency modes are all perfectly resonant in the cavity. The interaction Hamiltonian for this coupled nonlinear process can be written as [15]

$$\hat{H}_I = i\hbar(\kappa_1\hat{a}_0\hat{a}_1^\dagger\hat{a}_2^\dagger + \kappa_2\hat{a}_0\hat{a}_1\hat{a}_3^\dagger + \kappa_3\hat{a}_0\hat{a}_2\hat{a}_4^\dagger) + \mathrm{H.c.}, \quad (1)$$

where $\hat{a}_0$, $\hat{a}_1$, $\hat{a}_2$, $\hat{a}_3$, $\hat{a}_4$ are annihilation operators of the cavity modes corresponding to the frequency ω_0, ω_1, ω_2, ω_3, ω_4, respectively. κ_1, κ_2, and κ_3 are dimensionless nonlinear coupling coefficients of three nonlinear processes, which are related to the nonlinear susceptibility and structure parameters of the superlattice and taken as real without loss of generality [8,16].

III. THRESHOLD PROPERTIES AND OUTPUT FIELDS

In this section, we drive the output fields in the formalism of the semiclassical input-output transformation for the quantum fluctuations [17]. First, we derive the stationary solutions by solving the classical equations for the mean values of the fields. Second, we perform the stability analysis to determine the validity of the linearization method. Third, we employ the linearization method to solve the classical equations for fields to obtain the fluctuations.

The classical equations of motion for the fields inside the cavity are [18]

$$\tau\frac{d\alpha_0}{dt} = -\gamma_0\alpha_0 - \kappa_1\alpha_1\alpha_2 - \kappa_2\alpha_1^*\alpha_3 - \kappa_3\alpha_2^*\alpha_4 + \sqrt{2\gamma_0}\alpha_0^{in},$$

$$\tau\frac{d\alpha_1}{dt} = -\gamma_1\alpha_1 + \kappa_1\alpha_0\alpha_2^* - \kappa_2\alpha_0^*\alpha_3 + \sqrt{2\gamma_1}\alpha_1^{in},$$

$$\tau\frac{d\alpha_2}{dt} = -\gamma_2\alpha_2 + \kappa_1\alpha_0\alpha_1^* - \kappa_3\alpha_0^*\alpha_4 + \sqrt{2\gamma_2}\alpha_2^{in},$$

$$\tau\frac{d\alpha_3}{dt} = -\gamma_3\alpha_3 + \kappa_2\alpha_0\alpha_1 + \sqrt{2\gamma_3}\alpha_3^{in},$$

$$\tau\frac{d\alpha_4}{dt} = -\gamma_4\alpha_4 + \kappa_3\alpha_0\alpha_2 + \sqrt{2\gamma_4}\alpha_4^{in}, \quad (2)$$

where τ is the round-trip time of the light in the cavity and assumed to be the same value for all five modes. α_i $(i=0,1,2,3,4)$ are the intracavity field of frequency ω_i, respectively, α_i^{in} the input field of the cavity, γ_i the dimensionless damping rate which is related to the amplitude reflection and transmission coefficients of the input and the output couplers of the optical cavity.

Let $\alpha_i=\bar{\alpha}_i+\delta\alpha_i$, $\alpha_i^{in}=\bar{\alpha}_i^{in}+\delta\alpha_i^{in}$ $(i=0,1,2,3,4)$ where $\bar{\alpha}_i$ and $\bar{\alpha}_i^{in}$ are mean values of α_i and α_i^{in}. The source terms for the signal, idler, and sum-frequency modes have zero mean values: they are vacuum field $\alpha_i^{in}=\delta\alpha_i^{in}$ $(i=1,2,3,4)$. The pump field is assumed as a coherent field, its fluctuations are the same as the vacuum fluctuations.

Neglecting all fluctuations and correlations, we have the equations for the mean values [19],

$$\tau\frac{d\bar{\alpha}_0}{dt} = \gamma_0(\epsilon-\bar{\alpha}_0) - \kappa_1\bar{\alpha}_1\bar{\alpha}_2 - \kappa_2\bar{\alpha}_1^*\bar{\alpha}_3 - \kappa_3\bar{\alpha}_2^*\bar{\alpha}_4,$$

$$\tau\frac{d\bar{\alpha}_1}{dt} = -\gamma_1\bar{\alpha}_1 + \kappa_1\bar{\alpha}_0\bar{\alpha}_2^* - \kappa_2\bar{\alpha}_0^*\bar{\alpha}_3,$$

$$\tau\frac{d\bar{\alpha}_2}{dt} = -\gamma_2\bar{\alpha}_2 + \kappa_1\bar{\alpha}_0\bar{\alpha}_1^* - \kappa_3\bar{\alpha}_0^*\bar{\alpha}_4,$$

$$\tau\frac{d\bar{\alpha}_3}{dt} = -\gamma_3\bar{\alpha}_3 + \kappa_2\bar{\alpha}_0\bar{\alpha}_1, \quad \tau\frac{d\bar{\alpha}_4}{dt} = -\gamma_4\bar{\alpha}_4 + \kappa_3\bar{\alpha}_0\bar{\alpha}_2, \tag{3}$$

where ϵ is the pump amplitude which is taken to be real. The stationary solutions are obtained by setting $d\bar{\alpha}_i/dt=0$ $(i=0,1,2,3,4)$. We find that the solutions are divided into two classes depending on whether the system has an oscillation threshold or not.

We find that the system has a threshold if $\kappa_1 \geq \sqrt{\gamma_2/\gamma_3}\kappa_2 + \sqrt{\gamma_1/\gamma_4}\kappa_3$. When there is only one sum-frequency generation in this system, the above relation reduces to $\kappa_1 > \sqrt{\gamma_2/\gamma_3}\kappa_2$, which has been derived by Pennarun *et al.* [11]. The condition in our system requires a large nonlinear coupling coefficient of the down-conversion process κ_1, small nonlinear coupling coefficients of two sum-frequency generations κ_2, κ_3, and small damping rates of the signal and the idler modes γ_1 and γ_2. All these enable the signal and the idler modes to be macroscopically occupied if the pump amplitude ϵ is above the threshold. The value of the threshold is

$$\epsilon_c = \sqrt{\frac{\gamma_3\gamma_4\kappa_1^2 - \gamma_2\gamma_4\kappa_2^2 - \gamma_1\gamma_3\kappa_3^2 - \sqrt{(\gamma_3\gamma_4\kappa_1^2 - \gamma_2\gamma_4\kappa_2^2 - \gamma_1\gamma_3\kappa_3^2)^2 - 4\gamma_1\gamma_2\gamma_3\gamma_4\kappa_2^2\kappa_3^2}}{2\kappa_2^2\kappa_3^2}}. \tag{4}$$

We also find another critical value of the pump amplitude,

$$\epsilon_c' = \sqrt{\frac{\gamma_3\gamma_4\kappa_1^2 - \gamma_2\gamma_4\kappa_2^2 - \gamma_1\gamma_3\kappa_3^2 + \sqrt{(\gamma_3\gamma_4\kappa_1^2 - \gamma_2\gamma_4\kappa_2^2 - \gamma_1\gamma_3\kappa_3^2)^2 - 4\gamma_1\gamma_2\gamma_3\gamma_4\kappa_2^2\kappa_3^2}}{2\kappa_2^2\kappa_3^2}}. \tag{5}$$

When $\epsilon_c < \epsilon \leq \epsilon_c'$, there is only one set of nonzero solutions for all five modes. If $\epsilon > \epsilon_c'$, there will be two sets of nonzero solutions for all five modes. The analytical expressions of stationary solutions for different values of the pump amplitude ϵ when there exists a threshold are

(i) $\epsilon \leq \epsilon_c$

$$\bar{\alpha}_0 = \epsilon, \quad \bar{\alpha}_j = 0, \tag{6}$$

where $j=1,2,3,4$.

(ii) $\epsilon_c < \epsilon \leq \epsilon_c'$

$$\bar{\alpha}_0 = \epsilon_c,$$

$$\bar{\alpha}_2 = \pm\sqrt{\frac{\gamma_0\gamma_4(\gamma_1\gamma_3 + \kappa_2^2\bar{\alpha}_0^2)^2(\epsilon - \bar{\alpha}_0)}{\bar{\alpha}_0[\kappa_1^2\gamma_3\gamma_4(\gamma_1\gamma_3 + 2\kappa_2^2\bar{\alpha}_0^2) + \kappa_3(\gamma_1\gamma_3 + \kappa_2^2\bar{\alpha}_0^2)^2]}}e^{i\theta},$$

$$\bar{\alpha}_1 = \frac{\kappa_1\gamma_3\bar{\alpha}_0\bar{\alpha}_2}{\gamma_1\gamma_3 + \kappa_2^2\bar{\alpha}_0^2}e^{-i2\theta}, \quad \bar{\alpha}_3 = \frac{\kappa_2}{\gamma_3}\bar{\alpha}_0\bar{\alpha}_1, \quad \bar{\alpha}_4 = \frac{\kappa_3}{\gamma_4}\bar{\alpha}_0\bar{\alpha}_2, \tag{7}$$

where θ is an undetermined phase.

(iii) $\epsilon > \epsilon_c'$

$$\bar{\alpha}_0 = \epsilon_c \quad \text{or} \quad \bar{\alpha}_0 = \epsilon_c',$$

$$\bar{\alpha}_2 = \pm\sqrt{\frac{\gamma_0\gamma_4(\gamma_1\gamma_3 + \kappa_2^2\bar{\alpha}_0^2)^2(\epsilon - \bar{\alpha}_0)}{\bar{\alpha}_0[\kappa_1^2\gamma_3\gamma_4(\gamma_1\gamma_3 + 2\kappa_2^2\bar{\alpha}_0^2) + \kappa_3(\gamma_1\gamma_3 + \kappa_2^2\bar{\alpha}_0^2)^2]}}e^{i\theta'},$$

$$\bar{\alpha}_1 = \frac{\kappa_1\gamma_3\bar{\alpha}_0\bar{\alpha}_2}{\gamma_1\gamma_3 + \kappa_2^2\bar{\alpha}_0^2}e^{-i2\theta'}, \quad \bar{\alpha}_3 = \frac{\kappa_2}{\gamma_3}\bar{\alpha}_0\bar{\alpha}_1, \quad \bar{\alpha}_4 = \frac{\kappa_3}{\gamma_4}\bar{\alpha}_0\bar{\alpha}_2, \tag{8}$$

where θ' is an undetermined phase.

If $\kappa_1 < \sqrt{\gamma_2/\gamma_3}\kappa_2 + \sqrt{\gamma_1/\gamma_4}\kappa_3$, we find that there is no threshold in this system. On this condition the signal and the idler modes will not be macroscopically occupied however large the pump amplitude is. The analytical expressions of the stationary solutions when a threshold does not exist are

$$\bar{\alpha}_0 = \epsilon, \quad \bar{\alpha}_j = 0, \tag{9}$$

where $j=1,2,3,4$.

In Eqs. (2), we can linearize the fluctuations around the steady state to obtain

$$\tau\frac{d\delta\alpha_0}{dt} = -\gamma_0\delta\alpha_0 - \kappa_1\bar{\alpha}_2\delta\alpha_1 - \kappa_1\bar{\alpha}_1\delta\alpha_2 - \kappa_2\bar{\alpha}_3\delta\alpha_1^* - \kappa_2\bar{\alpha}_1^*\delta\alpha_3 - \kappa_3\bar{\alpha}_4\delta\alpha_2^* - \kappa_3\bar{\alpha}_2^*\delta\alpha_4 + \sqrt{2\gamma_0}\delta\alpha_0^{\text{in}},$$

$$\tau\frac{d\delta\alpha_1}{dt} = -\gamma_1\delta\alpha_1 + \kappa_1\bar{\alpha}_2^*\delta\alpha_0 + \kappa_1\bar{\alpha}_0\delta\alpha_2^* - \kappa_2\bar{\alpha}_3\delta\alpha_0^* - \kappa_2\bar{\alpha}_0^*\delta\alpha_3 + \sqrt{2\gamma_1}\delta\alpha_1^{\text{in}},$$

$$\tau\frac{d\delta\alpha_2}{dt} = -\gamma_2\delta\alpha_2 + \kappa_1\bar{\alpha}_1^*\delta\alpha_0 + \kappa_1\bar{\alpha}_0\delta\alpha_1^* - \kappa_3\bar{\alpha}_4\delta\alpha_0^* - \kappa_3\bar{\alpha}_0^*\delta\alpha_4 + \sqrt{2\gamma_2}\delta\alpha_2^{\text{in}},$$

$$\tau\frac{d\delta\alpha_3}{dt} = -\gamma_3\delta\alpha_3 + \kappa_2\bar{\alpha}_1\delta\alpha_0 + \kappa_2\bar{\alpha}_0\delta\alpha_1 + \sqrt{2\gamma_3}\delta\alpha_3^{\text{in}},$$

$$\tau\frac{d\delta\alpha_4}{dt} = -\gamma_4\delta\alpha_4 + \kappa_3\bar{\alpha}_2\delta\alpha_0 + \kappa_3\bar{\alpha}_0\delta\alpha_2 + \sqrt{2\gamma_4}\delta\alpha_4^{\text{in}}. \tag{10}$$

Equations (10) and their conjugate equations can be written together in a matrix form as

$$\tau\frac{d}{dt}\delta\tilde{\alpha} = -\mathbf{A}\,\delta\tilde{\alpha} + \mathbf{B}\,\delta\tilde{\alpha}^{\text{in}}, \tag{11}$$

where

$$\delta\tilde{\alpha} = [\delta\alpha_0 \;\; \delta\alpha_0^* \;\; \delta\alpha_1 \;\; \delta\alpha_1^*\delta\alpha_2 \;\; \delta\alpha_2^* \;\; \delta\alpha_3 \;\; \delta\alpha_3^*\delta\alpha_4 \;\; \delta\alpha_4^*]^T, \tag{12}$$

$$\delta\tilde{\alpha}^{\text{in}} = [\delta\alpha_0^{\text{in}} \;\; \delta\alpha_0^{\text{in}*} \;\; \delta\alpha_1^{\text{in}} \;\; \delta\alpha_1^{\text{in}*} \;\; \delta\alpha_2^{\text{in}} \;\; \delta\alpha_2^{\text{in}*} \;\; \delta\alpha_3^{\text{in}} \;\; \delta\alpha_3^{\text{in}*} \;\; \delta\alpha_4^{\text{in}} \;\; \delta\alpha_4^{\text{in}*}]^T, \tag{13}$$

$$\mathbf{A} = \begin{bmatrix}
\gamma_0 & 0 & \kappa_1\bar{\alpha}_2 & \kappa_2\bar{\alpha}_3 & \kappa_1\bar{\alpha}_1 & \kappa_3\bar{\alpha}_4 & \kappa_2\bar{\alpha}_1^* & 0 & \kappa_3\bar{\alpha}_2^* & 0 \\
0 & \gamma_0 & \kappa_2\bar{\alpha}_3^* & \kappa_1\bar{\alpha}_2^* & \kappa_3\bar{\alpha}_4^* & \kappa_1\bar{\alpha}_1^* & 0 & \kappa_2\bar{\alpha}_1 & 0 & \kappa_3\bar{\alpha}_2 \\
-\kappa_1\bar{\alpha}_2^* & \kappa_2\bar{\alpha}_3 & \gamma_1 & 0 & 0 & -\kappa_1\bar{\alpha}_0 & \kappa_2\bar{\alpha}_0^* & 0 & 0 & 0 \\
\kappa_2\bar{\alpha}_3^* & -\kappa_1\bar{\alpha}_2 & 0 & \gamma_1 & -\kappa_1\bar{\alpha}_0^* & 0 & 0 & \kappa_2\bar{\alpha}_0 & 0 & 0 \\
-\kappa_1\bar{\alpha}_1^* & \kappa_3\bar{\alpha}_4 & 0 & -\kappa_1\bar{\alpha}_0 & \gamma_2 & 0 & 0 & 0 & \kappa_3\bar{\alpha}_0^* & 0 \\
\kappa_3\bar{\alpha}_4^* & -\kappa_1\bar{\alpha}_1 & -\kappa_1\bar{\alpha}_0^* & 0 & 0 & \gamma_2 & 0 & 0 & 0 & \kappa_3\bar{\alpha}_0 \\
-\kappa_2\bar{\alpha}_1 & 0 & -\kappa_2\bar{\alpha}_0 & 0 & 0 & 0 & \gamma_3 & 0 & 0 & 0 \\
0 & -\kappa_2\bar{\alpha}_1^* & 0 & -\kappa_2\bar{\alpha}_0^* & 0 & 0 & 0 & \gamma_3 & 0 & 0 \\
-\kappa_3\bar{\alpha}_2 & 0 & 0 & 0 & -\kappa_3\bar{\alpha}_0 & 0 & 0 & 0 & \gamma_4 & 0 \\
0 & -\kappa_3\bar{\alpha}_2^* & 0 & 0 & 0 & -\kappa_3\bar{\alpha}_0^* & 0 & 0 & 0 & \gamma_4
\end{bmatrix}, \tag{14}$$

$$\mathbf{B} = \begin{bmatrix}
\sqrt{2\gamma_0} & 0 & 0 & 0 & 0 & 0 & 0 & 0 & 0 & 0 \\
0 & \sqrt{2\gamma_0} & 0 & 0 & 0 & 0 & 0 & 0 & 0 & 0 \\
0 & 0 & \sqrt{2\gamma_1} & 0 & 0 & 0 & 0 & 0 & 0 & 0 \\
0 & 0 & 0 & \sqrt{2\gamma_1} & 0 & 0 & 0 & 0 & 0 & 0 \\
0 & 0 & 0 & 0 & \sqrt{2\gamma_2} & 0 & 0 & 0 & 0 & 0 \\
0 & 0 & 0 & 0 & 0 & \sqrt{2\gamma_2} & 0 & 0 & 0 & 0 \\
0 & 0 & 0 & 0 & 0 & 0 & \sqrt{2\gamma_3} & 0 & 0 & 0 \\
0 & 0 & 0 & 0 & 0 & 0 & 0 & \sqrt{2\gamma_3} & 0 & 0 \\
0 & 0 & 0 & 0 & 0 & 0 & 0 & 0 & \sqrt{2\gamma_4} & 0 \\
0 & 0 & 0 & 0 & 0 & 0 & 0 & 0 & 0 & \sqrt{2\gamma_4}
\end{bmatrix}. \tag{15}$$

A is the drift matrix.

However, the validity of the linearization method requires that all the eigenvalues of the drift matrix **A** have a positive real part. In general, the eigenvalues of the drift matrix of this system are not easily obtained. In order to make a clear illustration of the characteristics of the system, we choose the special case that $\gamma_1=\gamma_2=\gamma_3=\gamma_4=\gamma$ and $\kappa_2=\kappa_3$. In the region below threshold and the region without threshold, the mean value of intracavity field has the same stationary solutions $\bar{\alpha}_0=\epsilon$, $\bar{\alpha}_j=0$ $(j=1,2,3,4)$. Simple analytical expressions of the eigenvalues of the drift matrix can be obtained in these two regions,

$$\lambda_{1,2} = \gamma_0,$$

$$\lambda_{3,4} = \frac{1}{2}(2\gamma - \epsilon\kappa_1 - \epsilon\sqrt{\kappa_1^2 - 4\kappa_2^2}),$$

$$\lambda_{5,6} = \frac{1}{2}(2\gamma + \epsilon\kappa_1 - \epsilon\sqrt{\kappa_1^2 - 4\kappa_2^2}),$$

$$\lambda_{7,8} = \frac{1}{2}(2\gamma - \epsilon\kappa_1 + \epsilon\sqrt{\kappa_1^2 - 4\kappa_2^2}),$$

$$\lambda_{9,10} = \frac{1}{2}(2\gamma + \epsilon\kappa_1 + \epsilon\sqrt{\kappa_1^2 - 4\kappa_2^2}). \quad (16)$$

In the regime with threshold, we have $\kappa_1 \geq 2\kappa_2$ and the threshold value is now

$$\epsilon_c = \frac{2\gamma}{\kappa_1 + \sqrt{\kappa_1^2 - 4\kappa_2^2}}. \quad (17)$$

In the region below threshold, we readily find that all the eigenvalues have a positive real part as $\epsilon < \epsilon_c$. In the region above threshold when $\epsilon \geq \epsilon_c$, however, we find that some eigenvalues do not have a positive real part so that the linearization method cannot be applied.

In the regime without threshold, we have $\kappa_1 < 2\kappa_2$. Inspection shows that all the eigenvalues have a positive real part if and only if $\epsilon < 2\gamma/\kappa_1$. We define here

$$\epsilon_c'' = \frac{2\gamma}{\kappa_1}. \quad (18)$$

Figure 2 is the plot of different stability regions, for $\gamma_0 = \gamma_1 = \gamma_2 = \gamma_3 = \gamma_4 = 0.02$ and $\kappa_2 = \kappa_3 = 0.05$, as κ_1 and ϵ are varied. It shows that only in the region under the solid line ϵ_c on the right (i.e., region below threshold) and the region under the dotted line ϵ_c'' on the left the system is stable so that linearization method can be applied. It is different from the case when there is only one sum-frequency generation (i.e., $\kappa_2 = 0$ or $\kappa_3 = 0$) [11]. Even in the regime without threshold this system will still become unstable when the pump amplitude is sufficiently large, just like in the regime with threshold. The linearized fluctuation analysis can be only carried out in the stable regions to calculate the quantum correlations. In the rest unstable regions, however, methods such as stochastic integration need to be employed. In this paper we shall only investigate the entanglement characteristics of the system in the stable regions.

Based upon the discussion above, we continue to use the linearization method to derive the fluctuations of the output fields in the two stable regions. Equation (11) can be solved in the frequency domain,

$$\delta\tilde{\alpha}(\omega) = (-i\omega\tau\mathbf{I} + \mathbf{A})^{-1}\mathbf{B}\,\delta\tilde{\alpha}^{\text{in}}(\omega), \quad (19)$$

where ω is the analysis frequency, and $\mathbf{I}$ is the unit matrix. Applying the boundary condition $\delta\tilde{\alpha}^{\text{out}} = \mathbf{B}\,\delta\tilde{\alpha} - \delta\tilde{\alpha}^{\text{in}}$ on the coupling mirror [15], where $\delta\tilde{\alpha}^{\text{out}}$ is the vector of output field fluctuations,

$$\delta\tilde{\alpha}^{\text{out}} = [\delta\alpha_0^{\text{out}}\ \ \delta\alpha_0^{\text{out}*}\ \ \delta\alpha_1^{\text{out}}\ \ \delta\alpha_1^{\text{out}*}\ \ \delta\alpha_2^{\text{out}}\ \ \delta\alpha_2^{\text{out}*}\ \ \delta\alpha_3^{\text{out}}\ \ \delta\alpha_3^{\text{out}*}\ \ \delta\alpha_4^{\text{out}}\ \ \delta\alpha_4^{\text{out}*}]^T, \quad (20)$$

we can get the output field fluctuations,

$$\delta\tilde{\alpha}^{\text{out}}(\omega) = [\mathbf{B}(-i\omega\tau\mathbf{I} + \mathbf{A})^{-1}\mathbf{B} - \mathbf{I}]\delta\tilde{\alpha}^{\text{in}}(\omega). \quad (21)$$

Now we have obtained the output field fluctuations and are ready to discuss the entanglement characteristics of the output fields, but before that we expect to calculate the number of photons in the four nonpump output modes, which is helpful in practical applications. Here we shall still confine our discussion to the two stable regions. From the steady-state solutions (6) and (9) we know that in these two stable regions the amplitude of the pump is much larger than that of the four nonpump modes, so undepleted pump approximation can be employed here, which yields the interaction Hamiltonian,

$$\hat{H}_I' = i\hbar e^{-i\omega_0 t}(\kappa_1 \hat{a}_1^\dagger \hat{a}_2^\dagger + \kappa_2 \hat{a}_1 \hat{a}_3^\dagger + \kappa_3 \hat{a}_2 \hat{a}_4^\dagger) + \text{H.c.} \quad (22)$$

Following the formalism which was obtained by Collett and Gardiner [15], the quantum Langevin equations for the four nonpump cavity modes are

$$\tau\frac{d\hat{a}_1}{dt} = -i\omega_1\tau\hat{a}_1 - \gamma_1\hat{a}_1 + \kappa_1 e^{-i\omega_0 t}\hat{a}_2^\dagger - \kappa_2 e^{i\omega_0 t}\hat{a}_3 + \sqrt{2\gamma_1}\hat{a}_1^{\text{in}},$$

$$\tau\frac{d\hat{a}_2}{dt} = -i\omega_2\tau\hat{a}_2 - \gamma_2\hat{a}_2 + \kappa_1 e^{-i\omega_0 t}\hat{a}_1^\dagger - \kappa_3 e^{i\omega_0 t}\hat{a}_4 + \sqrt{2\gamma_2}\hat{a}_2^{\text{in}},$$

$$\tau\frac{d\hat{a}_3}{dt} = -i\omega_3\tau\hat{a}_3 - \gamma_3\hat{a}_3 + \kappa_2 e^{-i\omega_0 t}\hat{a}_1 + \sqrt{2\gamma_3}\hat{a}_3^{\text{in}},$$

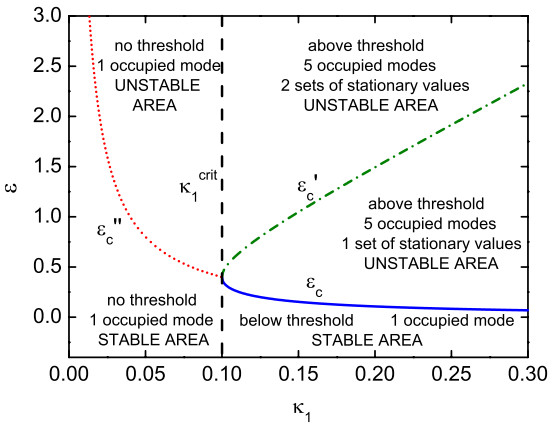

FIG. 2. (Color online) Stability of the stationary solutions with $\gamma_0 = \gamma_1 = \gamma_2 = \gamma_3 = \gamma_4 = 0.02$ and $\kappa_2 = \kappa_3 = 0.05$, as κ_1 and ϵ are varied. The dashed line κ_1^{crit} shows the separation between the regime with and without threshold.

$$\tau\frac{d\hat{a}_4}{dt} = -i\omega_4\tau\hat{a}_4 - \gamma_4\hat{a}_4 + \kappa_3 e^{-i\omega_0 t}\hat{a}_2 + \sqrt{2\gamma_4}\hat{a}_4^{\text{in}}, \quad (23)$$

where $\hat{a}_i^{\text{in}}$ $(i=1,2,3,4)$ are annihilation operators of the input fields and other symbols are defined the same as before. This is a set of linear equations. We transform to a rotating frame with

$$\hat{a}_i \to e^{i\omega_i t}\hat{a}_i, \quad i=1,2,3,4, \quad (24)$$

and similarly for the input operators. In matrix notation, the equations become

$$\tau\frac{d}{dt}\tilde{\hat{a}} = -\mathbf{A}'\tilde{\hat{a}} + \mathbf{B}'\tilde{\hat{a}}^{in}, \quad (25)$$

where

$$\tilde{\hat{a}} = [\hat{a}_1\ \hat{a}_1^\dagger\ \hat{a}_2\ \hat{a}_2^\dagger\ \hat{a}_3\ \hat{a}_3^\dagger\ \hat{a}_4\ \hat{a}_4^\dagger]^T, \quad (26)$$

$$\tilde{\hat{a}}^{\text{in}} = [\hat{a}_1^{\text{in}}\ \hat{a}_1^{\text{in}\dagger}\ \hat{a}_2^{\text{in}}\ \hat{a}_2^{\text{in}\dagger}\ \hat{a}_3^{\text{in}}\ \hat{a}_3^{\text{in}\dagger}\ \hat{a}_4^{\text{in}}\ \hat{a}_4^{\text{in}\dagger}]^T, \quad (27)$$

$$\mathbf{A}' = \begin{bmatrix} \gamma_1 & 0 & 0 & -\kappa_1 & \kappa_2 & 0 & 0 & 0 \\ 0 & \gamma_1 & -\kappa_1 & 0 & 0 & \kappa_2 & 0 & 0 \\ 0 & -\kappa_1 & \gamma_2 & 0 & 0 & 0 & \kappa_3 & 0 \\ -\kappa_1 & 0 & 0 & \gamma_2 & 0 & 0 & 0 & \kappa_3 \\ -\kappa_2 & 0 & 0 & 0 & \gamma_3 & 0 & 0 & 0 \\ 0 & -\kappa_2 & 0 & 0 & 0 & \gamma_3 & 0 & 0 \\ 0 & 0 & -\kappa_3 & 0 & 0 & 0 & \gamma_4 & 0 \\ 0 & 0 & 0 & -\kappa_3 & 0 & 0 & 0 & \gamma_4 \end{bmatrix}, \quad (28)$$

$$\mathbf{B}' = \begin{bmatrix} \sqrt{2\gamma_1} & 0 & 0 & 0 & 0 & 0 & 0 & 0 \\ 0 & \sqrt{2\gamma_1} & 0 & 0 & 0 & 0 & 0 & 0 \\ 0 & 0 & \sqrt{2\gamma_2} & 0 & 0 & 0 & 0 & 0 \\ 0 & 0 & 0 & \sqrt{2\gamma_2} & 0 & 0 & 0 & 0 \\ 0 & 0 & 0 & 0 & \sqrt{2\gamma_3} & 0 & 0 & 0 \\ 0 & 0 & 0 & 0 & 0 & \sqrt{2\gamma_3} & 0 & 0 \\ 0 & 0 & 0 & 0 & 0 & 0 & \sqrt{2\gamma_4} & 0 \\ 0 & 0 & 0 & 0 & 0 & 0 & 0 & \sqrt{2\gamma_4} \end{bmatrix}. \quad (29)$$

Equation (25) can be solved in the frequency domain,

$$\tilde{\hat{a}}(\omega) = (-i\omega\tau\mathbf{I} + \mathbf{A}')^{-1}\mathbf{B}'\tilde{\hat{a}}^{\text{in}}(\omega). \quad (30)$$

Applying the boundary condition $\tilde{\hat{a}}^{\text{out}} = \mathbf{B}'\tilde{\hat{a}} - \tilde{\hat{a}}^{\text{in}}$ on the coupling mirror, where

$$\tilde{\hat{a}}^{\text{out}} = [\hat{a}_1^{\text{out}}\ \hat{a}_1^{\text{out}\dagger}\ \hat{a}_2^{\text{out}}\ \hat{a}_2^{\text{out}\dagger}\ \hat{a}_3^{\text{out}}\ \hat{a}_3^{\text{out}\dagger}\ \hat{a}_4^{\text{out}}\ \hat{a}_4^{\text{out}\dagger}]^T, \quad (31)$$

$\hat{a}_i^{\text{out}}$, $\hat{a}_i^{\text{out}\dagger}$ $(i=1,2,3,4)$ are annihilation and creation operators of the output fields, we obtain the output operators,

$$\tilde{\hat{a}}^{\text{out}}(\omega) = [\mathbf{B}'(-i\omega\tau\mathbf{I} + \mathbf{A}')^{-1}\mathbf{B}' - \mathbf{I}]\tilde{\hat{a}}^{\text{in}}(\omega). \quad (32)$$

As the analytical expression of the solution (32) is quite complicated, we proceed on two additional assumptions to estimate the number of photons in the output modes. First, we assume that

$$\gamma_1 = \gamma_2, \quad \gamma_3 = \gamma_4, \quad \kappa_2 = \kappa_3. \quad (33)$$

It should be noted that after these symmetric parameters have been chosen the signal mode $\hat{a}_1$ is equivalent to the idler mode $\hat{a}_2$ and the two sum-frequency modes $\hat{a}_3$, $\hat{a}_4$ are equivalent to each other. For this reason we shall only show calculation for mode $\hat{a}_1$ and mode $\hat{a}_3$ next. Second, we assume that all the nonlinear coupling coefficients are much smaller than the damping rates,

$$\kappa_1, \kappa_2, \kappa_3 \ll \gamma_1, \gamma_2, \gamma_3, \gamma_4. \quad (34)$$

Therefore higher order terms of κ_1, κ_2, and κ_3 can be dropped in the calculation. On these two assumptions simple analytical results can be obtained from the solution (32),

$$\hat{a}_1^{\text{out}}(\omega_1+\omega) = C_{11}(\omega)\hat{a}_1^{\text{in}}(\omega_1+\omega) + C_{12}(\omega)\hat{a}_2^{\text{in}\dagger}(\omega_1-\omega) + C_{13}(\omega)\hat{a}_3^{\text{in}}(\omega_3+\omega) + C_{14}(\omega)\hat{a}_4^{\text{in}\dagger}(\omega_4-\omega),$$

$$\hat{a}_3^{\text{out}}(\omega_3+\omega)=C_{31}(\omega)\hat{a}_1^{\text{in}}(\omega_1+\omega)+C_{32}(\omega)\hat{a}_2^{\text{in}\dagger}(\omega_1-\omega)+C_{33}(\omega)\hat{a}_3^{\text{in}}(\omega_3+\omega)+C_{34}(\omega)\hat{a}_4^{\text{in}\dagger}(\omega_4-\omega), \tag{35}$$

with

$$C_{11}(\omega)=\frac{\gamma_1+i\omega\tau}{\gamma_1-i\omega\tau},\quad C_{12}(\omega)=\frac{2\gamma_1\kappa_1}{(\gamma_1-i\omega\tau)^2},$$

$$C_{13}(\omega)=-\frac{2\sqrt{\gamma_1\gamma_3}\kappa_2}{(\gamma_1-i\omega\tau)(\gamma_3-i\omega\tau)},$$

$$C_{14}(\omega)=-\frac{2\sqrt{\gamma_1\gamma_3}\kappa_1\kappa_2}{(\gamma_1-i\omega\tau)^2(\gamma_3-i\omega\tau)},$$

$$C_{31}(\omega)=\frac{2\sqrt{\gamma_1\gamma_3}\kappa_2}{(\gamma_1-i\omega\tau)(\gamma_3-i\omega\tau)},$$

$$C_{32}(\omega)=\frac{2\sqrt{\gamma_1\gamma_3}\kappa_1\kappa_2}{(\gamma_1-i\omega\tau)^2(\gamma_3-i\omega\tau)},$$

$$C_{33}(\omega)=\frac{\gamma_3+i\omega\tau}{\gamma_3-i\omega\tau},\quad C_{34}(\omega)=-\frac{2\gamma_3\kappa_1\kappa_2^2}{(\gamma_1-i\omega\tau)^2(\gamma_3-i\omega\tau)^2}. \tag{36}$$

The spectrum of the two output fields $S_1(\omega)$ and $S_3(\omega)$ are defined by [20],

$$\langle\hat{a}_1^{\text{out}\dagger}(\omega_1+\omega)\hat{a}_1^{\text{out}}(\omega_1+\omega')\rangle\equiv S_1(\omega)\delta(\omega-\omega'),$$

$$\langle\hat{a}_3^{\text{out}\dagger}(\omega_3+\omega)\hat{a}_3^{\text{out}}(\omega_3+\omega')\rangle\equiv S_3(\omega)\delta(\omega-\omega'). \tag{37}$$

They can be calculated from Eq. (35). The results are

$$S_1(\omega)=|C_{12}(\omega)|^2+|C_{14}(\omega)|^2=\frac{4\gamma_1^2\kappa_1^2}{(\omega^2\tau^2+\gamma_1^2)^2},$$

$$S_3(\omega)=|C_{32}(\omega)|^2+|C_{34}(\omega)|^2=\frac{4\gamma_1\gamma_3\kappa_1^2\kappa_2^2}{(\omega^2\tau^2+\gamma_1^2)^2(\omega^2\tau^2+\gamma_3^2)}. \tag{38}$$

Higher order terms of κ_1, κ_2, and κ_3 have been still dropped here. The photon rate of the output modes $\hat{a}_1^{\text{out}}$ and $\hat{a}_3^{\text{out}}$ can be calculated as

$$R_1=\langle\hat{E}_1^{\text{out}(-)}(t)\hat{E}_1^{\text{out}(+)(t)}\rangle=\frac{1}{2\pi}\int d\omega S_1(\omega),$$

$$R_3=\langle\hat{E}_3^{\text{out}(-)}(t)\hat{E}_3^{\text{out}(+)}(t)\rangle=\frac{1}{2\pi}\int d\omega S_3(\omega), \tag{39}$$

where

$$\hat{E}_1^{\text{out}(+)}(t)=[\hat{E}_1^{\text{out}(-)}(t)]^\dagger=\frac{1}{\sqrt{2\pi}}\int d\omega\hat{a}_1^{\text{out}}(\omega)e^{-i\omega t},$$

$$\hat{E}_3^{\text{out}(+)}(t)=[\hat{E}_3^{\text{out}(-)}(t)]^\dagger=\frac{1}{\sqrt{2\pi}}\int d\omega\hat{a}_3^{\text{out}}(\omega)e^{-i\omega t}. \tag{40}$$

From Eq. (38), we have

$$R_1=\frac{1}{2\pi}\int_{-\infty}^{\infty}d\omega\frac{4\gamma_1^2\kappa_1^2}{(\omega^2\tau^2+\gamma_1^2)^2}=\frac{\kappa_1^2}{\tau\gamma_1},$$

$$R_3=\frac{1}{2\pi}\int_{-\infty}^{\infty}d\omega\frac{4\gamma_1\gamma_3\kappa_1^2\kappa_2^2}{(\omega^2\tau^2+\gamma_1^2)^2(\omega^2\tau^2+\gamma_3^2)}=\frac{(2\gamma_1+\gamma_3)\kappa_1^2\kappa_2^2}{\tau\gamma_1^2(\gamma_1+\gamma_3)^2}. \tag{41}$$

As analytical results of the output mode photon rates have been obtained in Eq. (41), we may now estimate their values in practical applications. The nonlinear coupling coefficients and damping rates in Eq. (41) are all dimensionless. The nonlinear coupling coefficient κ_1 and κ_2 can be also interpreted as single-pass gain parameters of the signal and sum-frequency photons, respectively. For we have confined our discussion to the two stable regions where the amplitude of the pump is much larger than that of the four nonpump modes, small signal approximation can be employed here. Therefore with perfect phase matching the nonlinear coupling coefficients can be written as

$$\kappa_1=\sqrt{\frac{8\omega_1\omega_2 I_0}{c^3\varepsilon_0 n_0 n_1 n_2}}L_{\text{PDC}}d,\quad \kappa_2=\sqrt{\frac{8\omega_1\omega_3 I_0}{c^3\varepsilon_0 n_0 n_1 n_3}}L_{\text{SFG1}}d, \tag{42}$$

where I_0 is the intensity of the pump, c the speed of light in vacuum, ε_0 the vacuum permittivity, n_0, n_1, n_2, and n_3 the refractive indexes of corresponding modes of light in the nonlinear medium, d the piezoelectric strain constant, L_{PDC} and L_{SFG1} the interaction length of the parametric down-conversion and one of the sum-frequency generation, respectively. With a pump intensity of 10 mW/(mm^2 s) and an interaction length of 10 mm, the value of the nonlinear coupling coefficients is typically 10^{-3}. On the other hand, the reciprocal of the damping rate is of the order of the number of bounces of light before it leaves the cavity. 10^{-2} is a reasonable value for the damping rate. At last, the round-trip time of the light in the cavity τ is about 10^{-10} s. Let $\kappa_1=\kappa_2=10^{-3}$, $\gamma_1=\gamma_3=10^{-2}$, $\tau=10^{-10}$ s in Eq. (41), where it should be noted that the chosen values agree with our assumption $\kappa_1,\kappa_2,\kappa_3\ll\gamma_1,\gamma_2,\gamma_3,\gamma_4$ in Eq. (34), we have the estimated values for the two output mode photon rates,

$$R_1\approx 10^6/\text{s},\quad R_3\approx 10^4/\text{s}. \tag{43}$$

It is shown by Eq. (43) that a reasonable amount of output mode photons can already be generated in this cavity system with just a low pump intensity of 10 mW/(mm^2 s). With a higher pump intensity or larger single-pass gain, we may certainly expect not only an increase in the amount of all the output photons but also a narrower gap between the amount of the sum-frequency photons and that of the signal or idler photons, which is helpful when measuring nonclassical properties among them. The above calculation of the photon rates

shows that this four mode generation scheme is quite feasible in practical applications and in Sec. IV we shall prove quadripartite entanglement among these four modes.

IV. CV QUADRIPARTITE ENTANGLEMENT CHARACTERISTICS

According to the sufficient inseparability criterion for CV multipartite entanglement which was proposed by van Loock and Furusawa [21], one of the sufficient inseparability criterion for CV genuine quadripartite entanglement among the four nonpump modes in this system contain these six inequalities,

$$\begin{aligned}
&\text{I} \quad S_{12} = \langle \delta^2(\hat{X}_1 - \hat{X}_2)\rangle + \langle \delta^2(\hat{Y}_1 + \hat{Y}_2 + g_3\hat{Y}_3 + g_4\hat{Y}_4)\rangle \geq 1,\\
&\text{II} \quad S_{13} = \langle \delta^2(\hat{X}_1 - \hat{X}_3)\rangle + \langle \delta^2(\hat{Y}_1 + g_2\hat{Y}_2 + \hat{Y}_3 + g_4\hat{Y}_4)\rangle \geq 1,\\
&\text{III} \quad S_{14} = \langle \delta^2(\hat{X}_1 - \hat{X}_4)\rangle + \langle \delta^2(\hat{Y}_1 + g_2\hat{Y}_2 + g_3\hat{Y}_3 + \hat{Y}_4)\rangle \geq 1,\\
&\text{IV} \quad S_{23} = \langle \delta^2(\hat{X}_2 - \hat{X}_3)\rangle + \langle \delta^2(g_1\hat{Y}_1 + \hat{Y}_2 + \hat{Y}_3 + g_4\hat{Y}_4)\rangle \geq 1,\\
&\text{V} \quad S_{24} = \langle \delta^2(\hat{X}_2 - \hat{X}_4)\rangle + \langle \delta^2(g_1\hat{Y}_1 + \hat{Y}_2 + g_3\hat{Y}_3 + \hat{Y}_4)\rangle \geq 1,\\
&\text{VI} \quad S_{34} = \langle \delta^2(\hat{X}_3 - \hat{X}_4)\rangle + \langle \delta^2(g_1\hat{Y}_1 + g_2\hat{Y}_2 + \hat{Y}_3 + \hat{Y}_4)\rangle \geq 1.
\end{aligned} \tag{44}$$

S_{12}, S_{13}, S_{14}, S_{23}, S_{24}, and S_{34} represent the quantum correlation spectra of the output field. $\hat{X}_i$ and $\hat{Y}_i$ $(i=1,2,3,4)$ are amplitude and phase quadrature operators of the output nonpump fields, respectively, which are defined as $\hat{X}_i=(\hat{a}_i^{\text{out}}+\hat{a}_i^{\text{out}\dagger})/2$ and $\hat{Y}_i=-i(\hat{a}_i^{\text{out}}-\hat{a}_i^{\text{out}\dagger})/2$. g_k $(k=1,2,3,4)$ are scaling factors which can be adjusted to minimize the correlation spectra.

If a multipartite system is partially separable, its density operator can be written in the form of a statistical mixture of reduced density operators of the subsystems. For a quadripartite system, there are seven kinds of partially separable forms, each of which leads to some of the inequalities in Eq. (44). Specifically, the following statements for (at least partially) separable states hold [21],

$$\begin{aligned}
&\hat{\rho} = \sum_i \eta_i \hat{\rho}_{i,123} \otimes \hat{\rho}_{i,4} \Rightarrow \text{III,V,VI},\\
&\hat{\rho} = \sum_i \eta_i \hat{\rho}_{i,124} \otimes \hat{\rho}_{i,3} \Rightarrow \text{II,IV,VI},\\
&\hat{\rho} = \sum_i \eta_i \hat{\rho}_{i,134} \otimes \hat{\rho}_{i,2} \Rightarrow \text{I,IV,V},\\
&\hat{\rho} = \sum_i \eta_i \hat{\rho}_{i,234} \otimes \hat{\rho}_{i,1} \Rightarrow \text{I,II,III},
\end{aligned} \tag{45}$$

and

$$\hat{\rho} = \sum_i \eta_i \hat{\rho}_{i,12} \otimes \hat{\rho}_{i,34} \Rightarrow \text{II,III,IV,V},$$

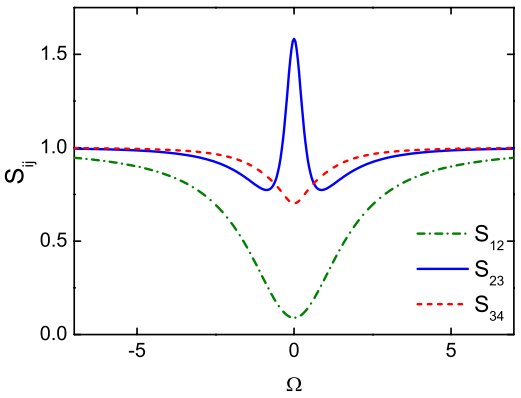

FIG. 3. (Color online) The quantum correlation spectra versus normalized analysis frequency $\Omega=\omega\tau/\gamma_1$ for the system below threshold with $\epsilon=0.5\epsilon_c$.

$$\hat{\rho} = \sum_i \eta_i \hat{\rho}_{i,13} \otimes \hat{\rho}_{i,24} \Rightarrow \text{I,III,IV,VI},$$

$$\hat{\rho} = \sum_i \eta_i \hat{\rho}_{i,14} \otimes \hat{\rho}_{i,23} \Rightarrow \text{I,II,V,VI}. \tag{46}$$

To verify the full inseparability of the quadripartite system, any of the partially separable forms above must be ruled out, which requires the violations of at least three inequalities in Eq. (44).

From the output field fluctuations obtained in Eq. (21), all correlation spectra can be readily calculated. Although analytical results for them is possible to derive, they are extremely unwieldy and not at all enlightening, even when simplified on some assumptions such as $\gamma_1=\gamma_2=\gamma_3=\gamma_4$ and $\kappa_2=\kappa_3$. We have therefore chosen to present the results graphically only. In this paper we have chosen to show three correlation spectra S_{12}, S_{23}, and S_{34}. It is sufficient to demonstrate genuine quadripartite entanglement with all these three spectra violating the inequality. As discussed in Sec. III, the stable regions were linearized fluctuation analysis can be applied are divided into two different classes: the region below threshold and the region without threshold. We shall analyze

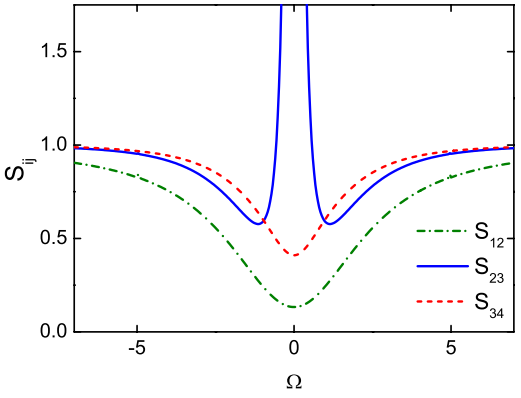

FIG. 4. (Color online) The quantum correlation spectra versus normalized analysis frequency $\Omega=\omega\tau/\gamma_1$ for the system below threshold with $\epsilon=0.9\epsilon_c$.

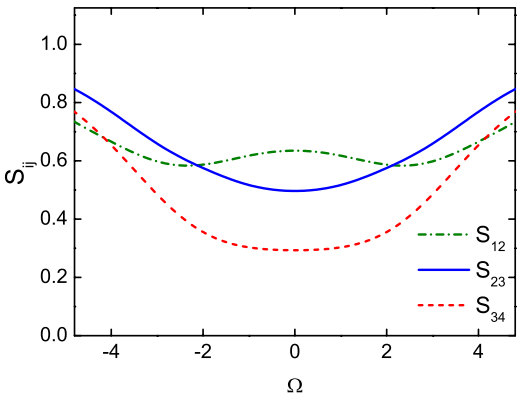

FIG. 5. (Color online) The quantum correlation spectra versus normalized analysis frequency $\Omega=\omega\tau/\gamma_1$ for the system without threshold with $\epsilon=1.5\epsilon_c^o$.

the entanglement characteristics in these two regions, respectively.

In Figs. 3 and 4, we plot the quantum correlation spectra versus normalized analysis frequency $\Omega=\omega\tau/\gamma_1$ for the system below threshold with $\epsilon=0.5\epsilon_c$ and $\epsilon=0.9\epsilon_c$ respectively. Other system parameters are set as $\gamma_0=0.02$, $\gamma_1=\gamma_2=0.005$, $\gamma_3=\gamma_4=0.025$, $\kappa_1=0.1$, and $\kappa_2=\kappa_3=0.1$. We see that in Fig. 3 S_{12}, S_{23}, and S_{34} violate the inequalities over quite a large frequency region, which is sufficient to prove the genuine quadripartite entanglement. Figure 4 shows that the violation of the inequalities has increased for all the spectra with the pump amplitude approaching the threshold, from $0.5\epsilon_c$ to $0.9\epsilon_c$.

In the analysis of entanglement characteristics in the regime without threshold, we particularly choose the parameters with which the system stays in the stable region where linearized fluctuation analysis can be applied, and for convenience we shall scale the pump amplitude ϵ by the normal optical parametric oscillator threshold $\epsilon_c^o=\sqrt{\gamma_1\gamma_2/\kappa_1}$. In Fig. 5, we show the quantum correlation spectra versus normalized analysis frequency $\Omega=\omega\tau/\gamma_1$ for the system without threshold with $\epsilon=1.5\epsilon_c^o$, $\gamma_0=0.02$, $\gamma_1=\gamma_2=0.01$, $\gamma_3=\gamma_4=0.04$, $\kappa_1=0.05$, and $\kappa_2=\kappa_3=0.1$. In the frequency range presented in Fig. 5, we see that almost all the spectra are

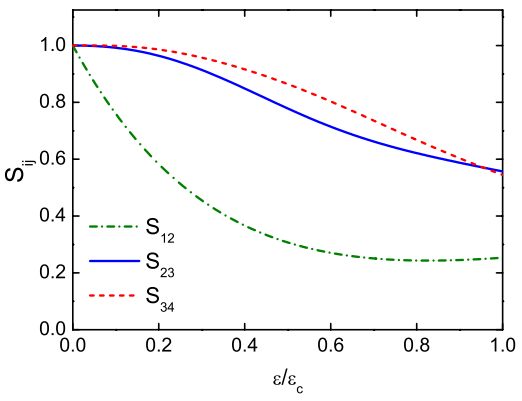

FIG. 6. (Color online) The quantum correlation spectra versus pump amplitude ϵ for the system below threshold with the normalized frequency $\Omega=\omega\tau/\gamma_1=1$.

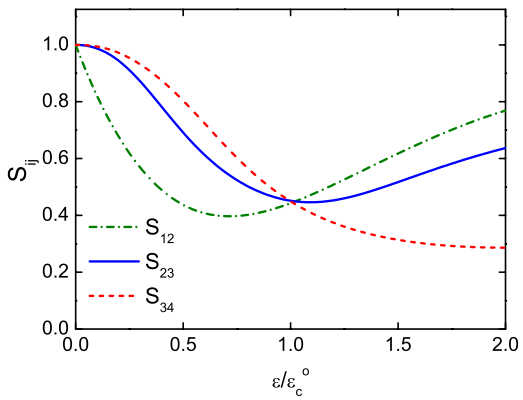

FIG. 7. (Color online) The quantum correlation spectra versus pump amplitude ϵ for the system without threshold with the normalized frequency $\Omega=\omega\tau/\gamma_1=1$.

below 1 and they all violate the inequality by quite a large amount, which may make it easier to experimentally verify the genuine quadripartite entanglement in the regime without threshold than the previous below threshold case.

We then analyze the quantum correlation spectra with varying pump amplitude ϵ. The quantum correlation spectra versus pump amplitude ϵ for the system below threshold are plotted in Fig. 6 with $\Omega=\omega\tau/\gamma_1=1$, $\gamma_0=0.02$, $\gamma_1=\gamma_2=0.005$, $\gamma_3=\gamma_4=0.025$, $\kappa_1=0.1$, and $\kappa_2=\kappa_3=0.1$. From Fig. 6 we can see that genuine quadripartite entanglement still exists as all the spectra show clear violation and maximal violation of the inequalities is achieved near the threshold. However, in the immediate neighborhood of the threshold, the calculated spectra are not accurate because of the invalidity of the linearized fluctuation analysis at the threshold point.

In Fig. 7, we show the quantum correlation spectra versus pump amplitude ϵ for the system without threshold with $\Omega=\omega\tau/\gamma_1=1$, $\gamma_0=0.02$, $\gamma_1=\gamma_2=0.01$, $\gamma_3=\gamma_4=0.04$, $\kappa_1=0.05$, and $\kappa_2=\kappa_3=0.1$. Clear evidence of genuine quadripartite entanglement can be seen in Fig. 7 and maximal violation of the inequalities is achieved around $\epsilon=\epsilon_c^o$.

At last, we investigate the effects of varying the down-conversion nonlinear coupling coefficient κ_1 in the system

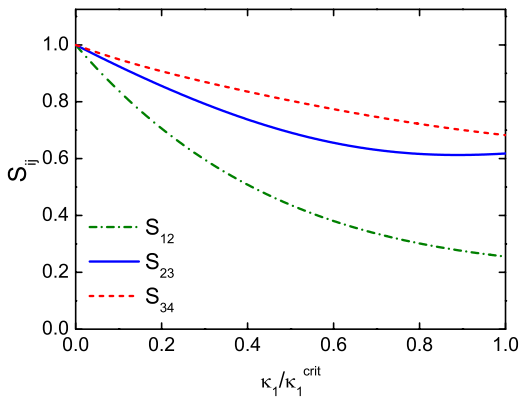

FIG. 8. (Color online) The quantum correlation spectra versus nonlinear coupling coefficient κ_1 for the system without threshold with the pump amplitude $\epsilon=0.5\epsilon_c^o$ and the normalized frequency $\Omega=\omega\tau/\gamma_1=1$.

without threshold. In Fig. 8, we plot the quantum correlation spectra versus nonlinear coupling coefficient κ_1 for the system without threshold with $\epsilon=0.5\epsilon_c^o$, $\Omega=\omega\tau/\gamma_1=1$, $\gamma_0=0.02$, $\gamma_1=\gamma_2=0.01$, $\gamma_3=\gamma_4=0.04$, and $\kappa_2=\kappa_3=0.1$. We can see that in the present range of κ_1 all spectra are below 1 and when κ_1 is near the critical value κ_1^{crit} maximal violation is achieved. It should be still noted that because of the invalidity of the linearized fluctuation analysis at the critical point the calculated spectra are not accurate in the immediate neighborhood of κ_1^{crit}.

V. CONCLUSION

We have proposed a scheme to generate continuous-variable genuine quadripartite entanglement based on intracavity parametric down-conversion cascaded with double sum-frequency generations. Unlike the case when there is only one sum-frequency generation cascaded with parametric down-conversion, we have found that even in the regime without threshold the system may still become unstable when the pump amplitude is sufficiently large. When the system is in stable regions, we have analyzed the quantum correlation spectra of the output field using the linearization method and theoretically proved genuine quadripartite entanglement among the four nonpump modes for a wide range of parameters. The scheme can be experimentally realized with an optical oscillator cavity in which a triperiodic or quasiperiodic optical superlattice is used as the nonlinear medium. Moreover, only one pump is needed and the frequencies of the entangled four modes can be different from one another. These features make the scheme a compact way to generate multicolor CV quadripartite entanglement, which may find a variety of applications in quantum information.

ACKNOWLEDGMENTS

This research is supported by the National Natural Science Foundation of China under Contracts No. 10534042 and No. 60578034 and the State Key Program for Basic Research of China (Grant No. 2004CB619003).

[1] P. van Loock and S. L. Braunstein, Phys. Rev. Lett. **84**, 3482 (2000).
[2] T. Aoki, N. Takei, H. Yonezawa, K. Wakui, T. Hiraoka, A. Furusawa, and P. van Loock, Phys. Rev. Lett. **91**, 080404 (2003).
[3] H. Yonezawa, T. Aoki, and A. Furusawa, Nature (London) **431**, 430 (2004).
[4] J. Zhang, C. Xie, and K. Peng, Phys. Rev. Lett. **95**, 170501 (2005).
[5] A. Furusawa, J. L. Sørensen, S. L. Braunstein, C. A. Fuchs, H. J. Kimble, and E. S. Polzik, Science **282**, 706 (1998).
[6] J. Jing, J. Zhang, Y. Yan, F. Zhao, C. Xie, and K. Peng, Phys. Rev. Lett. **90**, 167903 (2003).
[7] S. Tanzilli, W. Tittel, M. Halder, O. Alibart, P. Baldi, N. Gisin, and H. Zbinden, Nature **437**, 116 (2005).
[8] A. Ferraro, M. G. A. Paris, M. Bondani, A. Allevi, E. Puddu, and A. Andreoni, J. Opt. Soc. Am. B **21**, 1241 (2004).
[9] J. Guo, H. Zou, Z. Zhai, J. Zhang, and J. Gao, Phys. Rev. A **71**, 034305 (2005).
[10] Y. B. Yu, Z. D. Xie, X. Q. Yu, H. X. Li, P. Xu, H. M. Yao, and S. N. Zhu, Phys. Rev. A **74**, 042332 (2006).
[11] C. Pennarun, A. S. Bradley, and M. K. Olsen, Phys. Rev. A **76**, 063812 (2007).
[12] A. S. Bradley, M. K. Olsen, O. Pfister, and R. C. Pooser, Phys. Rev. A **72**, 053805 (2005).
[13] Z. D. Gao, S. N. Zhu, Shih-Yu Tu, and A. H. Kunga, Appl. Phys. Lett. **89**, 181101 (2006).
[14] X. Su, A. Tan, X. Jia, J. Zhang, C. Xie, and K. Peng, Phys. Rev. Lett. **98**, 070502 (2007).
[15] M. J. Collett and C. W. Gardiner, Phys. Rev. A **30**, 1386 (1984).
[16] Z. Y. Ou, S. F. Pereira, and H. J. Kimble, Appl. Phys. B: Lasers Opt. **55**, 265 (1992).
[17] S. Reynaud and A. Heidmann, Opt. Commun. **71**, 209 (1989).
[18] C. Fabre, E. Giacobino, A. Heidmann, L. Lugiato, S. Reynaud, M. Vadacchino, and Wang Kaige, Quantum Opt. **2**, 159 (1990).
[19] P. D. Drummond, K. J. McNeil, and D. F. Walls, Opt. Acta **27**, 321 (1980); **28**, 211 (1981).
[20] Y. J. Lu and Z. Y. Ou, Phys. Rev. A **62**, 033804 (2000).
[21] P. van Loock and A. Furusawa, Phys. Rev. A **67**, 052315 (2003).